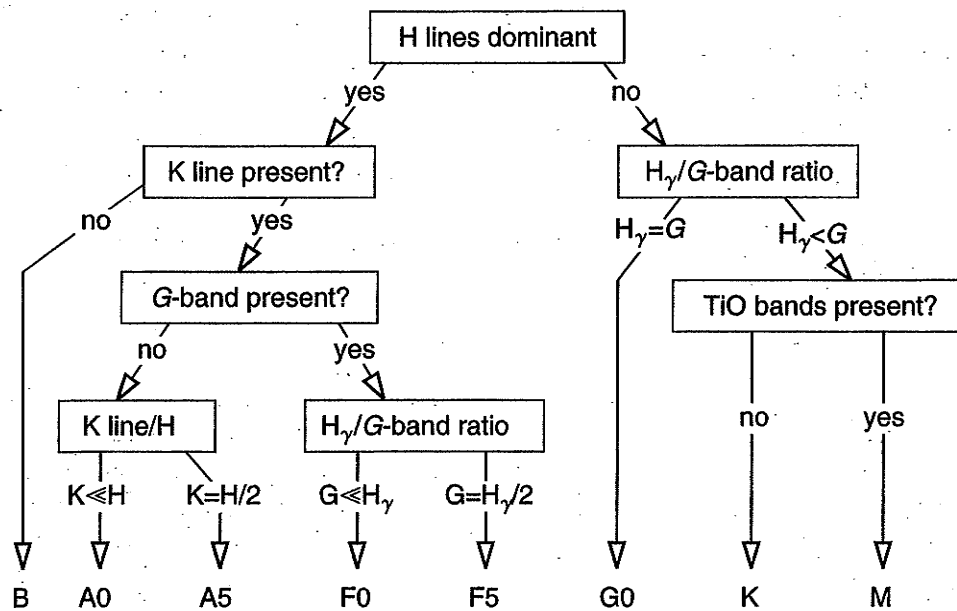


"Arm Chair"

# Spectral classification



Gray

Ca II H 3969  
K 3934

K H  
W

[illegible]

Figure 2.2 The Main Sequence from O4 to G2. Spectra in Figures 2.2–2.5 were obtained with the GM spectrograph on the 32" telescope of the Dark Sky Observatory. These rectified spectra have a resolution of  $3.6 \text{ \AA}$ , and have been offset by 0.7 continuum units for clarity.

[illegible]

Figure 2.4 Ib Supergiants from O7 to G0. These spectra are rectified, and have been offset vertically by 0.7 continuum units.

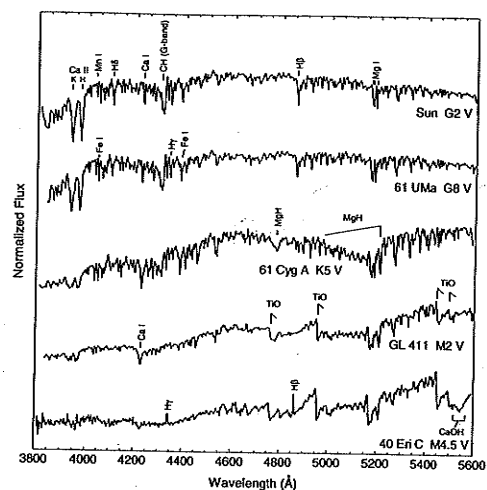


Figure 2.3 The Main Sequence from G2 to M4.5. These flux-calibrated spectra have been normalized at 5445 Å, and given integer vertical offsets for clarity.

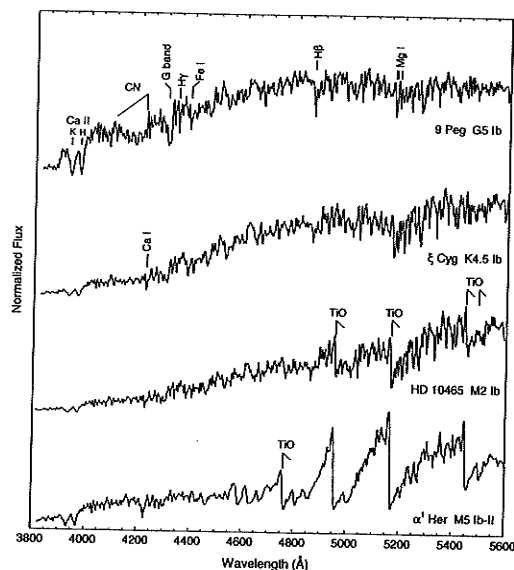
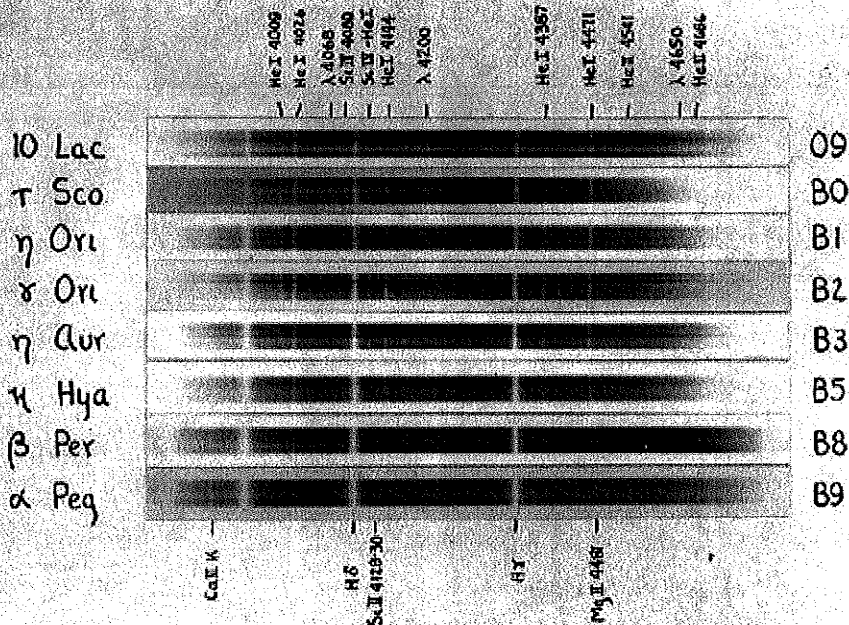


Figure 2.5 1b Supergiants from G5 to M5. These spectra are in normalized flux format, and have been given integer vertical offsets for clarity.

# Main Sequence 09-B9

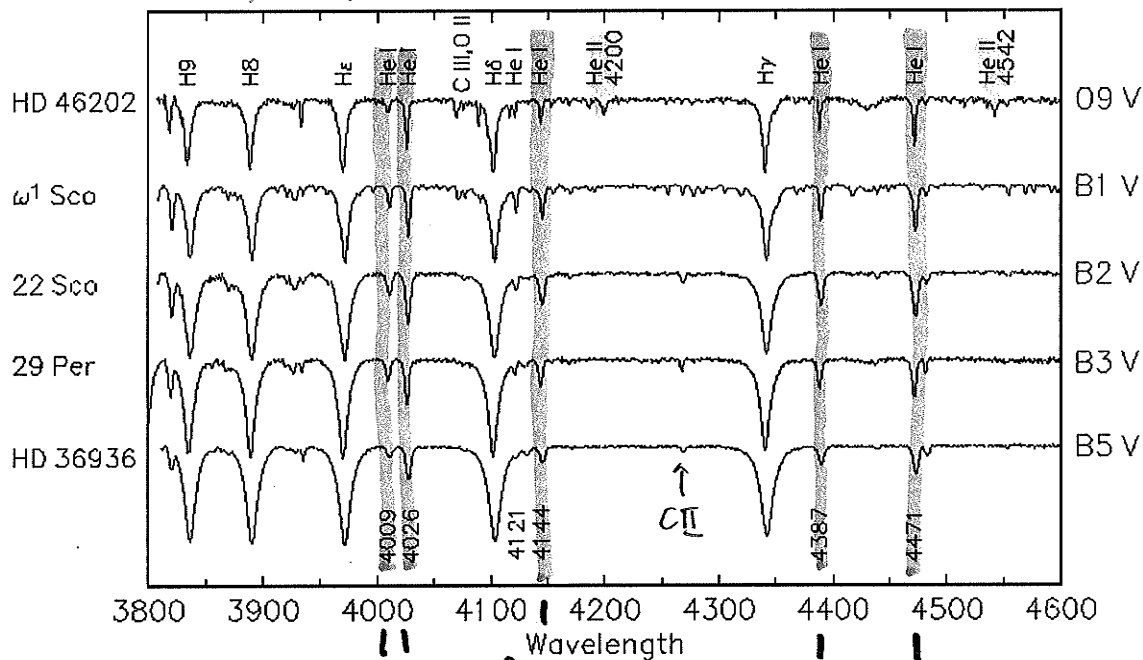


All of the above stars are of luminosity class V

Eastman Process

## Main Sequence 09 – B5

He I & Ca II confusion



• why are H lines increasing in strength?

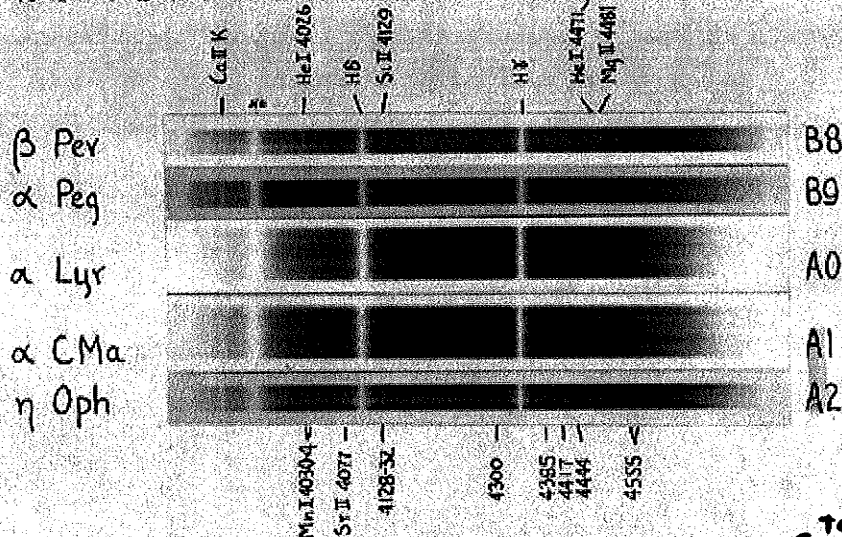
↑ He II increasing

He I maximize

ratio of He I lines key

## Main Sequence B8-A2

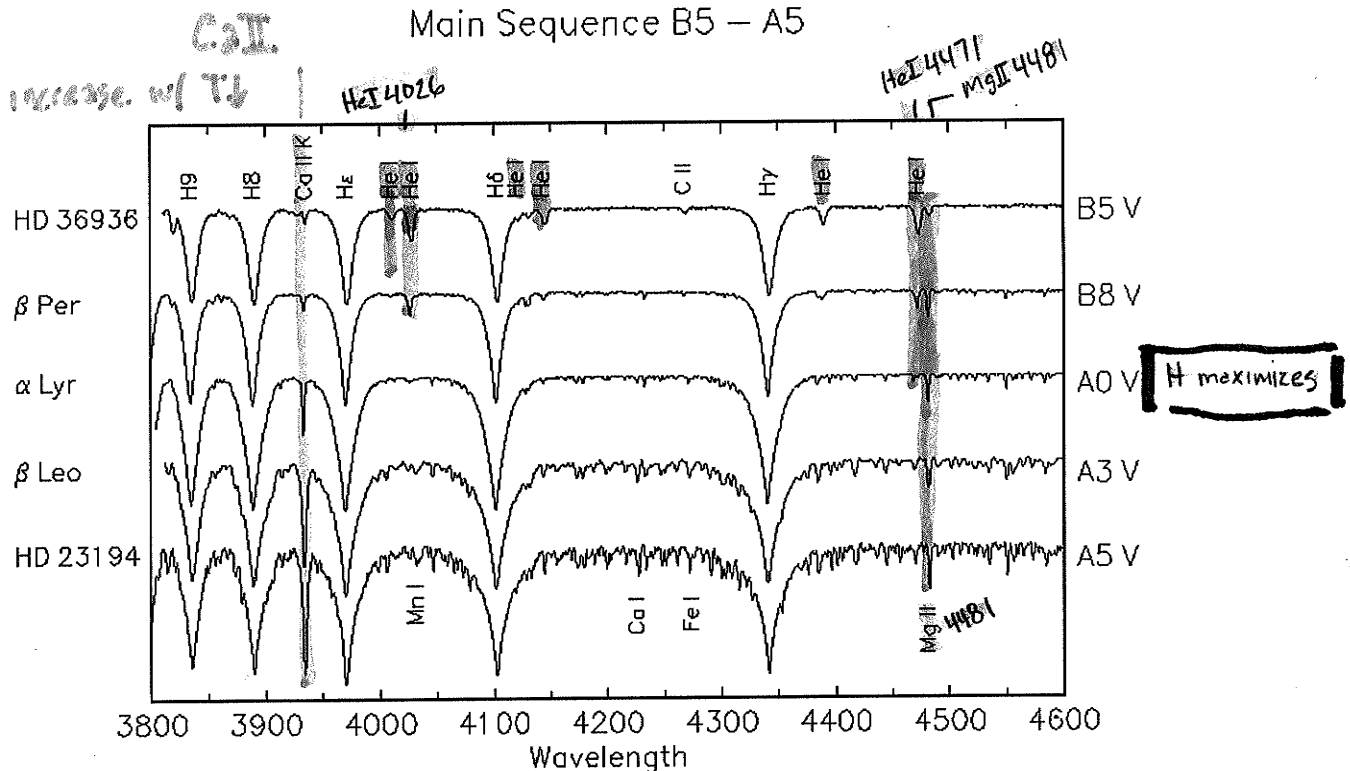
He I 4026, which is equal in intensity to K in the B8 dwarf  $\beta$  Per, becomes fainter at B9 and disappears at A0. In the B9 star  $\alpha$  Peg He I 4026 = Si II 4129. He I 4471 behaves similarly to He I 4026.



The singly ionized metallic lines are progressively stronger in  $\alpha$  CMa and  $\eta$  Oph than in  $\alpha$  Lyr. The spectral type is determined from the ratios: B8-B9: He I 4026:Ca II K, He I 4026:Si II 4129, He I 4471:Mg II 4481. A0-A2: Mg II 4481:4385, Si II 4129:Mn I 4030-4.

Eastman Process

## Main Sequence B5 - A5

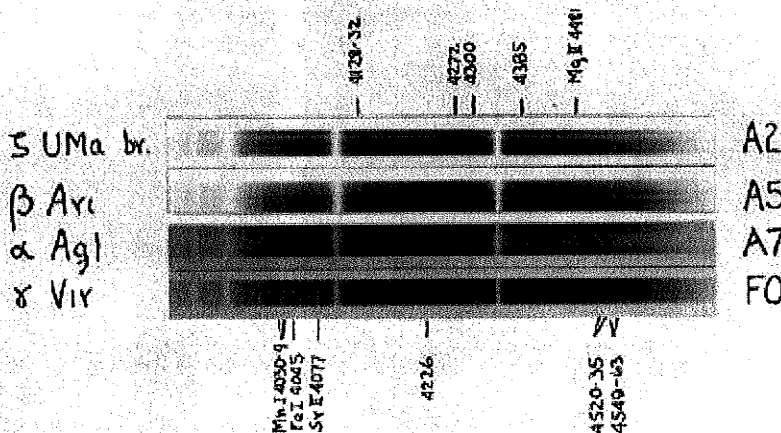


# Main Sequence A2-F0

The blends at  $\lambda\lambda$  4030-4 and 4300 increase rapidly in intensity from A2 to F0

G-band

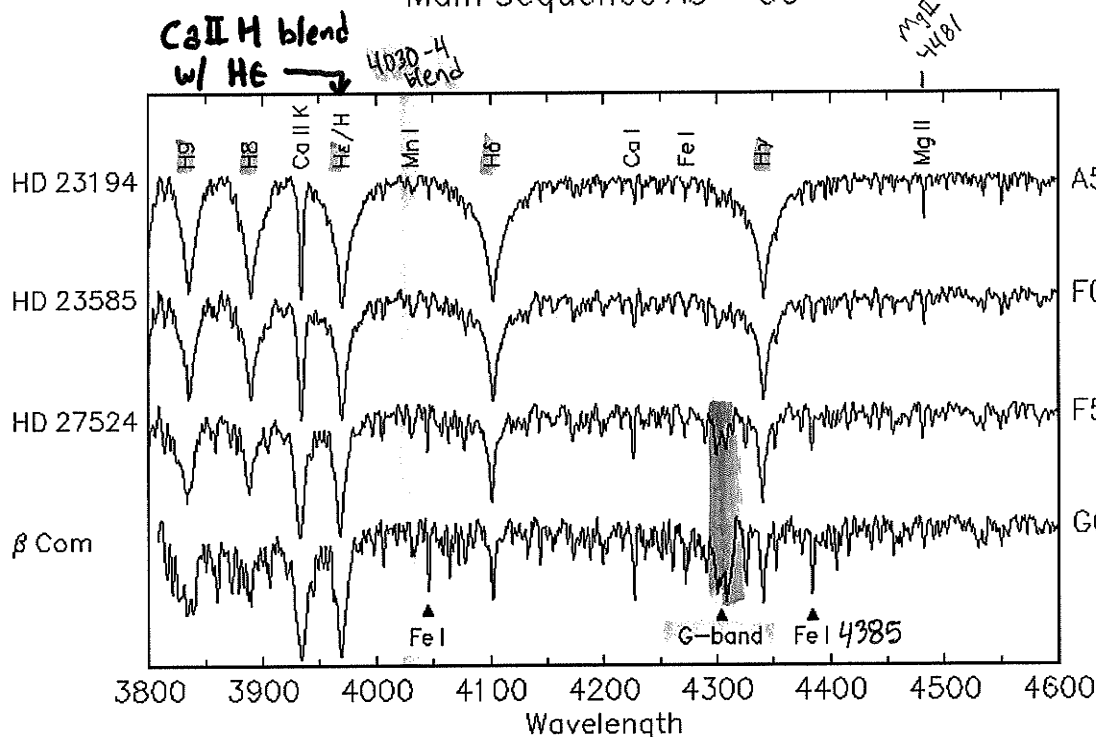
G-band is CH



The spectral type is determined from the ratios: Min I 4030-4 :  $\lambda$  4128-32,  $\lambda$  4300 : Fe I  $\lambda$  4385

Eastman Process

# Main Sequence A5 - G0

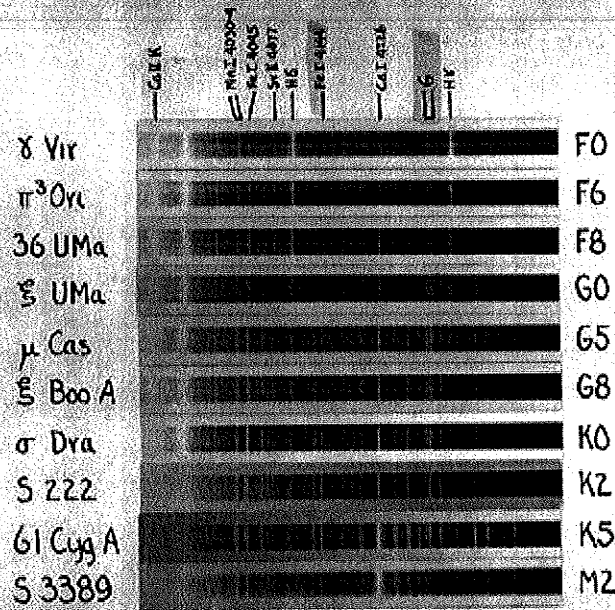


H $\gamma$  > G-band

G-band = H $\gamma$

G-band is CH

# Main Sequence F0-M2



as T decreases

growing

decreasing

Ca I 4226

H lines

Mg II 4030-4

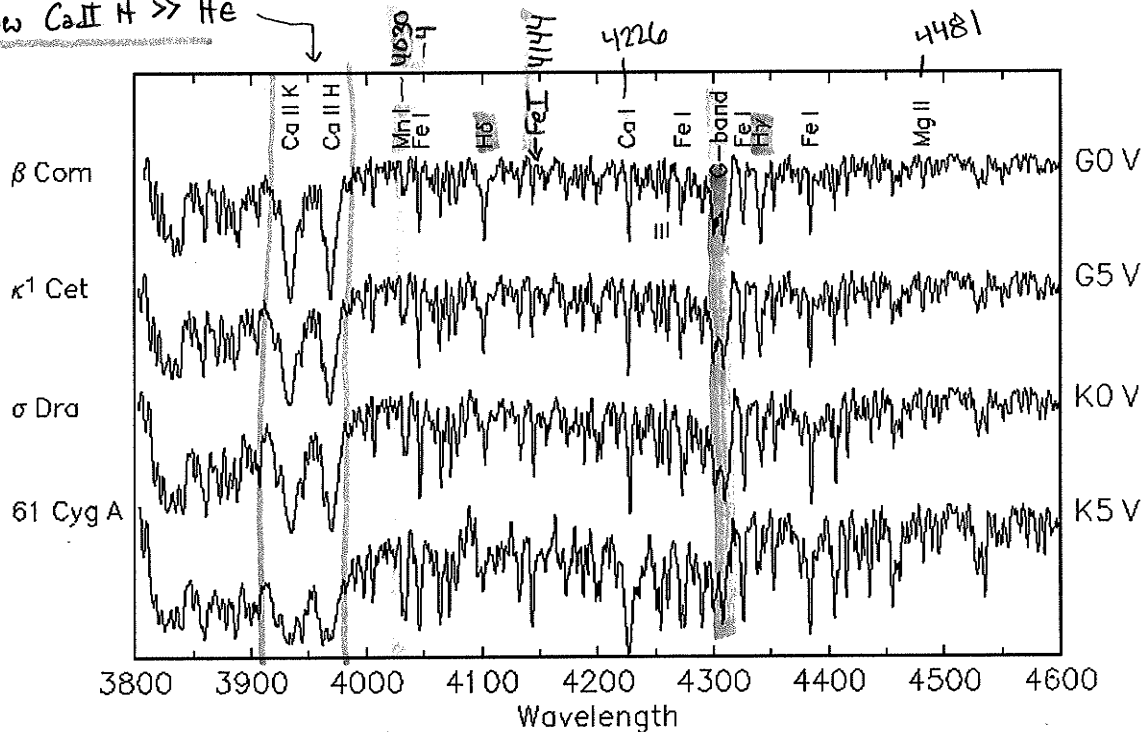
Hδ, Hε

G-band

All stars illustrated are of luminosity class V  
Cramer Hi-Speed Special.

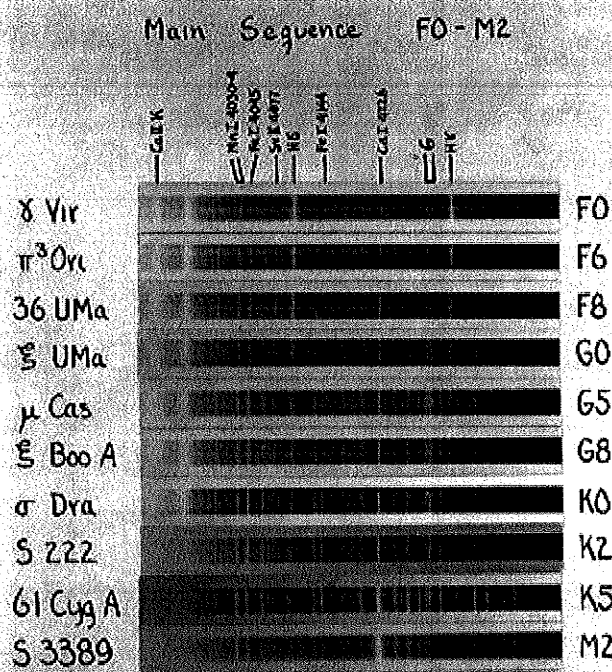
## Main Sequence G0 - K5

now Ca II H >> Hε



G-band  
> H<sub>γ</sub>

as T decreases



decreasing

CaII  
FeI 4144

increasing

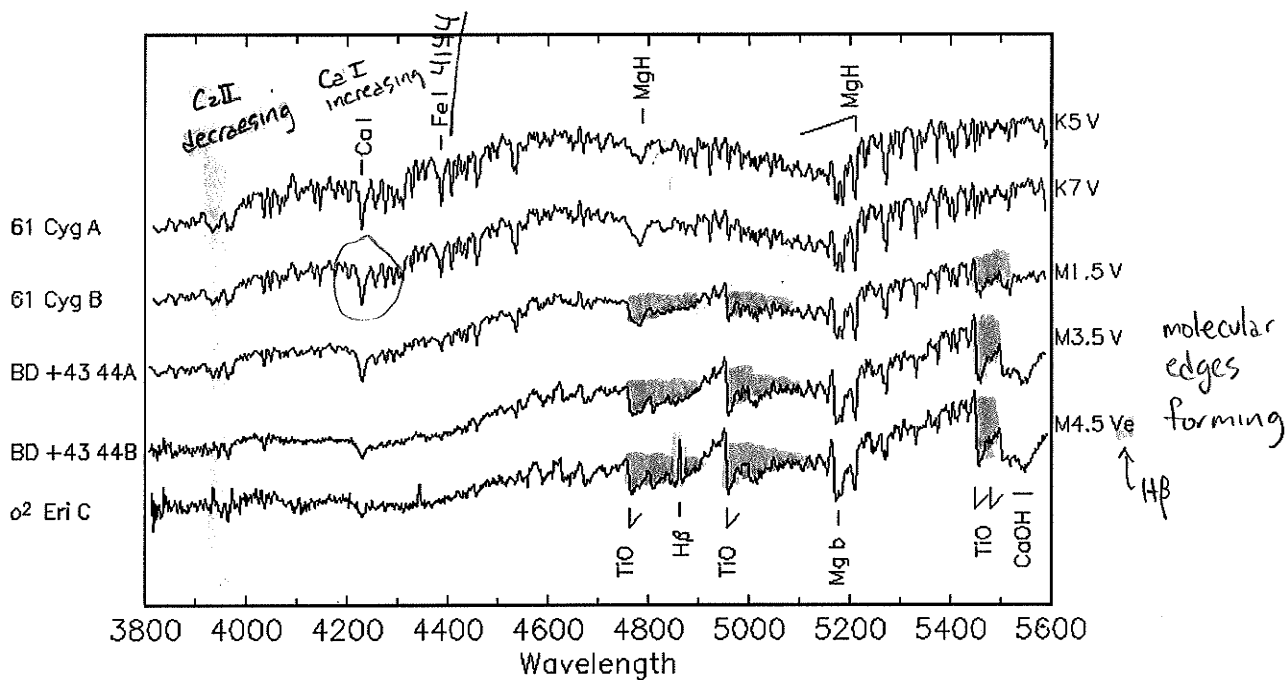
CaI  
TiO

MgH and TiO bands  
merge with cooling

{hydrogen  
lines are  
gone}

All stars illustrated are of luminosity class V  
 Cramer Hi-Speed Special

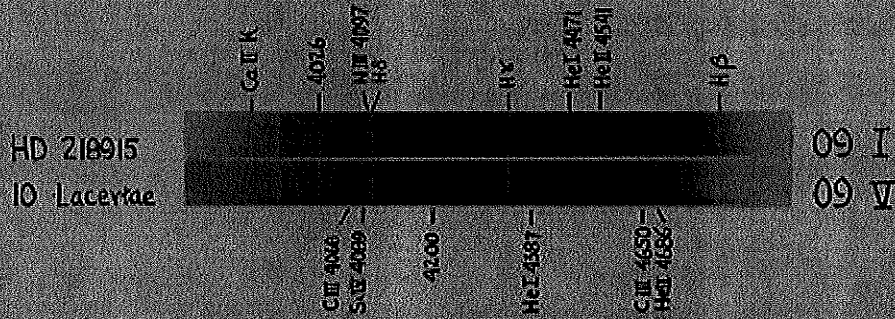
### Main Sequence K5 - M4.5 Normalized Flux





## Luminosity Effects at O9

HD 218915 appears to be a pronounced supergiant, while 10 Lacertae is an ordinary main sequence star



The spectral type is determined from the ratio  
He I 4471 : He II 4541

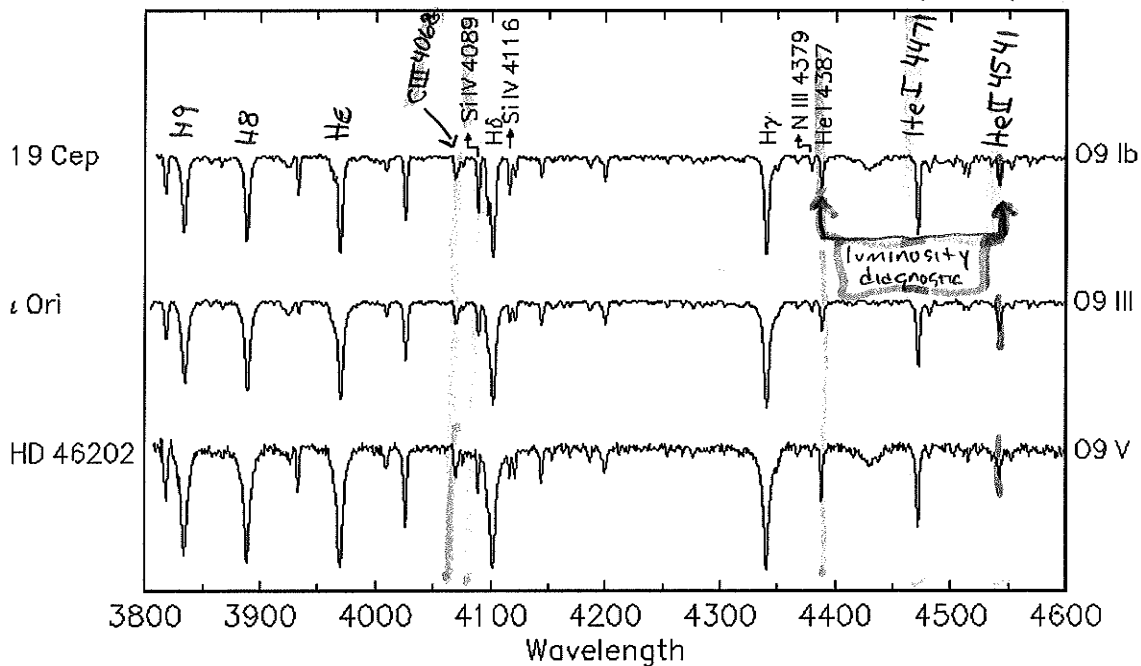
The difference in luminosity is shown by the ratios  
C III 4068 : Si IV 4089, He I 4387 : He II 4541 and  
C III 4650 : He II 4686

Cramer  
Hi-Speed

## Luminosity Effects at O9

diagnostic of luminosity class

diagnostic of spectral type



decreasing

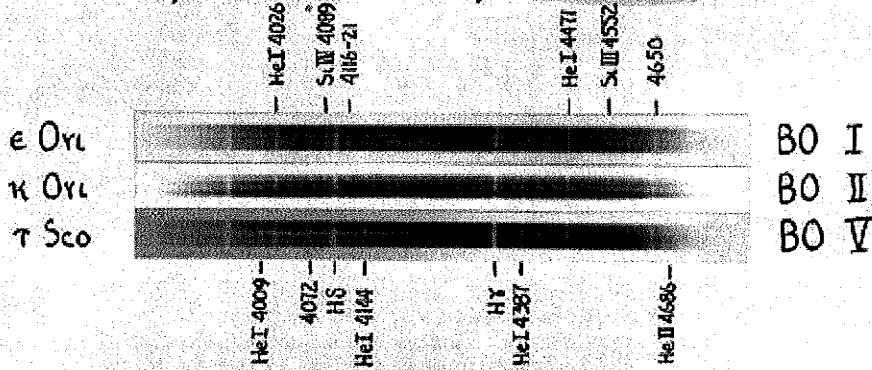
$\log(g)$

increasing



## Luminosity Effects at B0

Si II 4089 shows a progressive decrease in intensity on passing from the very luminous supergiant  $\epsilon$  Ori toward the main sequence star  $\tau$  Sco. The He I lines 4387, 4144 and 4009 have a negative absolute magnitude effect and are strongest in the dwarfs.



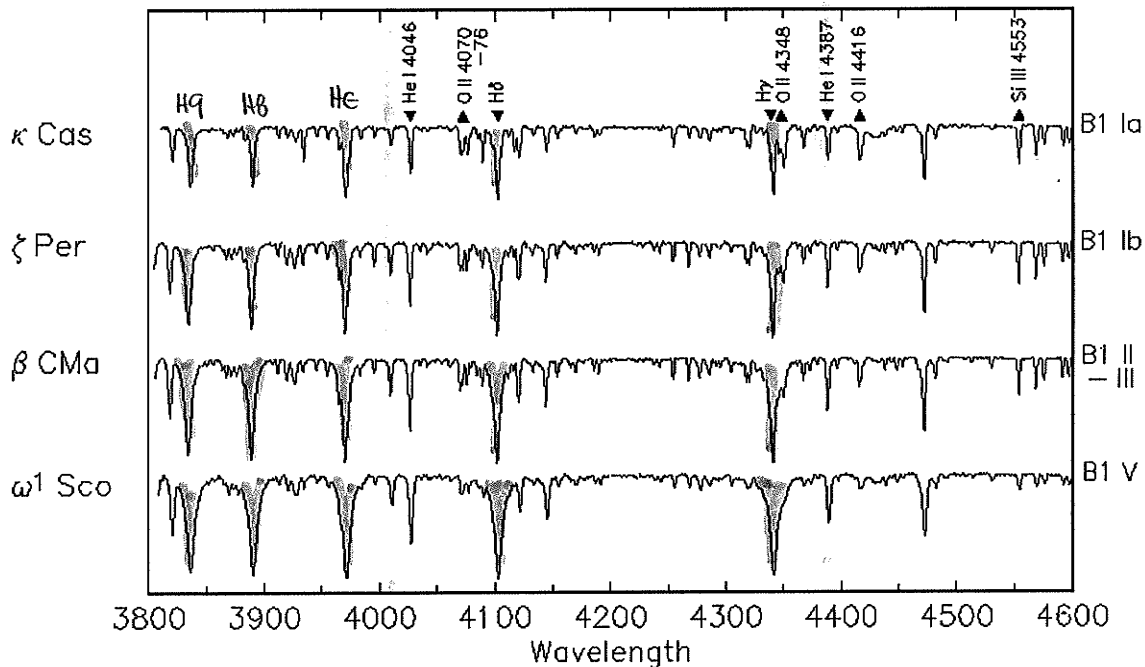
At class B0 the line at  $\lambda 4200$  is absent or very much fainter than He I 4387. Si II 4089 is stronger than Si III 4552. The following luminosity ratios are used: He I 4009: Si II 4089,  $\lambda 4072$ : Si II 4089, and  $\lambda 4119$ : He I 4144. The line He II 4686 is present in the dwarf, but is fainter than in class O9.5.

Eastman  
Process

why is hydrogen  
increasing from  
B1 Ia  $\rightarrow$  B1 V

## Luminosity Effects at B1

He I 4009 luminosity diagnostic  $\rightarrow$



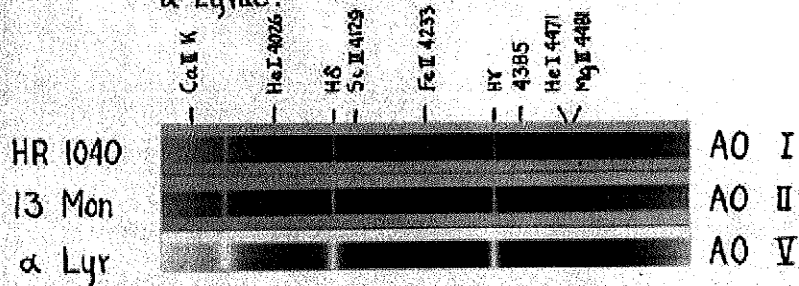
gravity  
decreasing

gravity  
increasing

## Luminosity Effects At A0

The H lines become progressively stronger on passing from the supergiant HR 1040 to the main sequence star  $\alpha$  Lyrae.

} pressure broadening

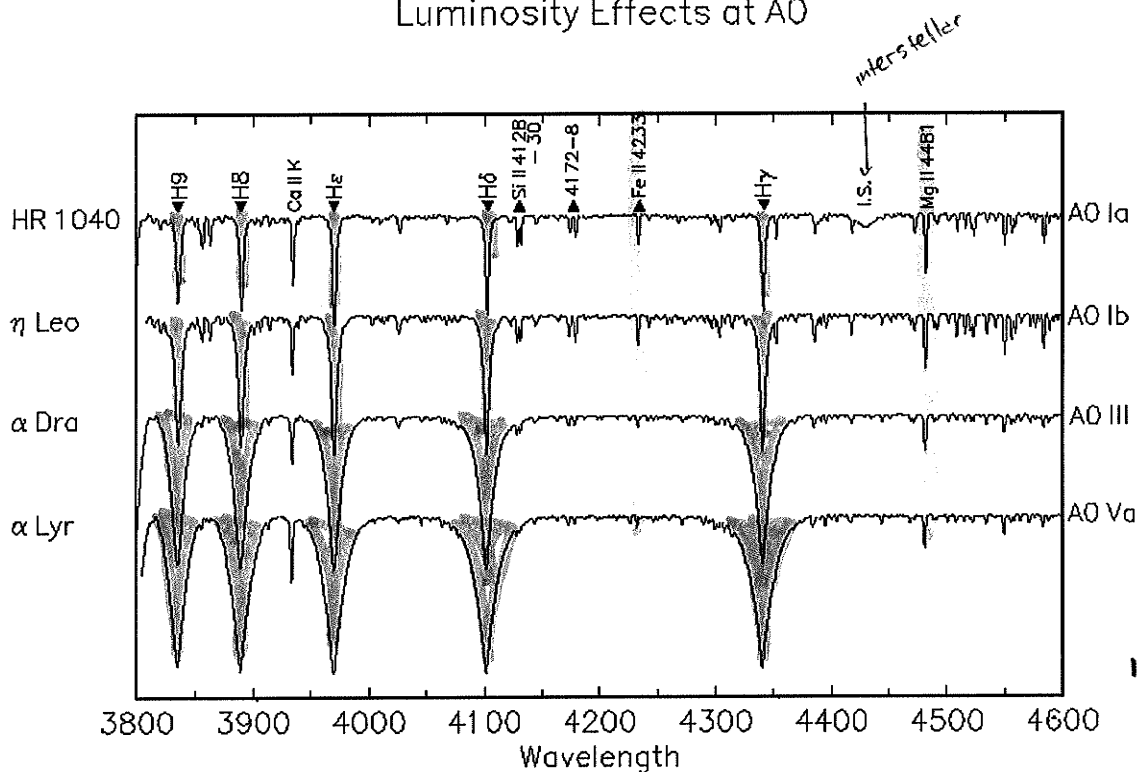


At A0 He I 4026 is faint or absent, and is weaker than Si II 4129. The lines of Fe II are strengthened in the supergiants.

Eastman Process

Now, we really see effects of pressure broadening

## Luminosity Effects at A0



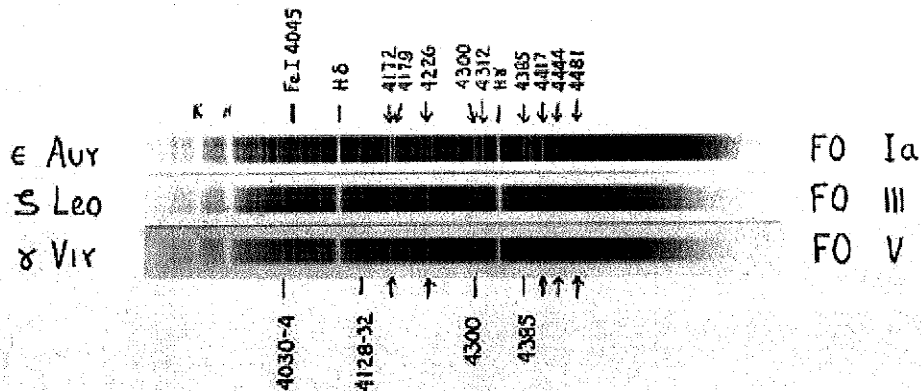
decreasing

$\log(g)$

increasing

## Luminosity Effects At F0

Luminosity differences are shown by the ratios 4417:4481, 4444:4481 and 4172:4226. A number of enhanced lines are strengthened in the spectrum of  $\epsilon$  Aurigae.



Giants (S Leo) and main sequence stars ( $\gamma$  Vir) are classified by the ratios 4030-4:4128-32 and 4300:4385. The classification of the supergiants is a special problem.  $\epsilon$  Aurigae is considered to be of class F0 from the intensity of the strong neutral metallic lines.

Eastman Process

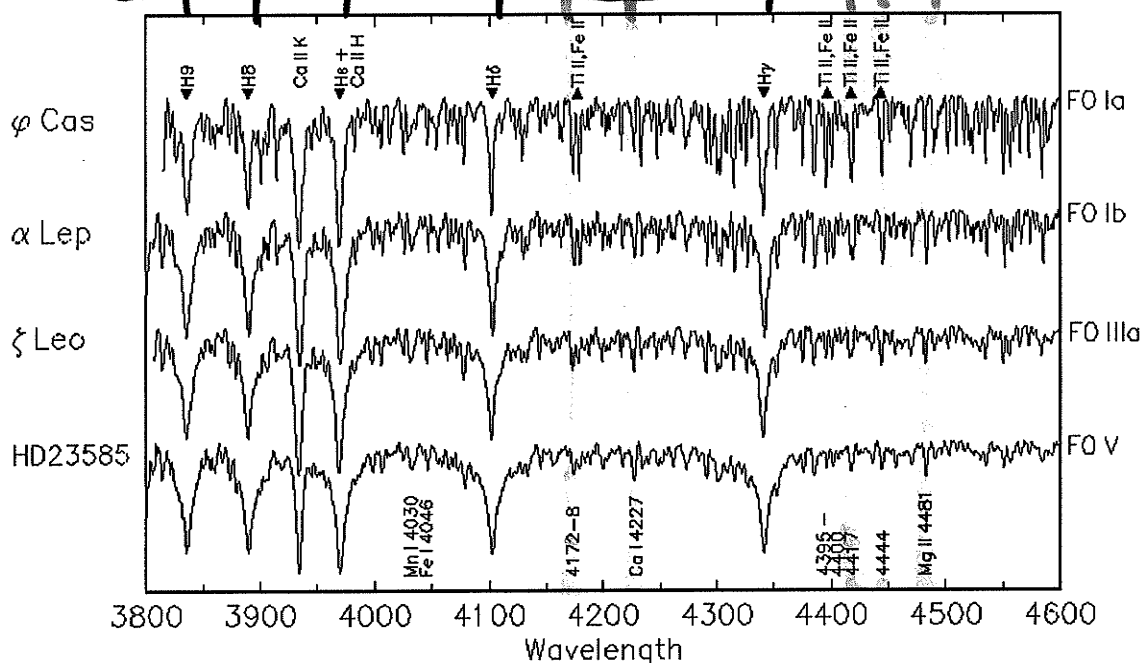
Why not use hydrogen for luminosity class diagnostics?

dust, changes line ratios  
- note that diagnostics are clustered in small  $\Delta\lambda$

## Luminosity Effects at F0

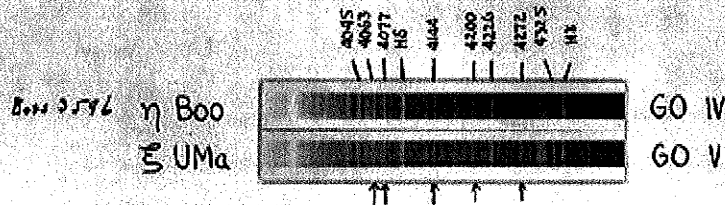
H lines (Balmer)

Luminosity diagnostics



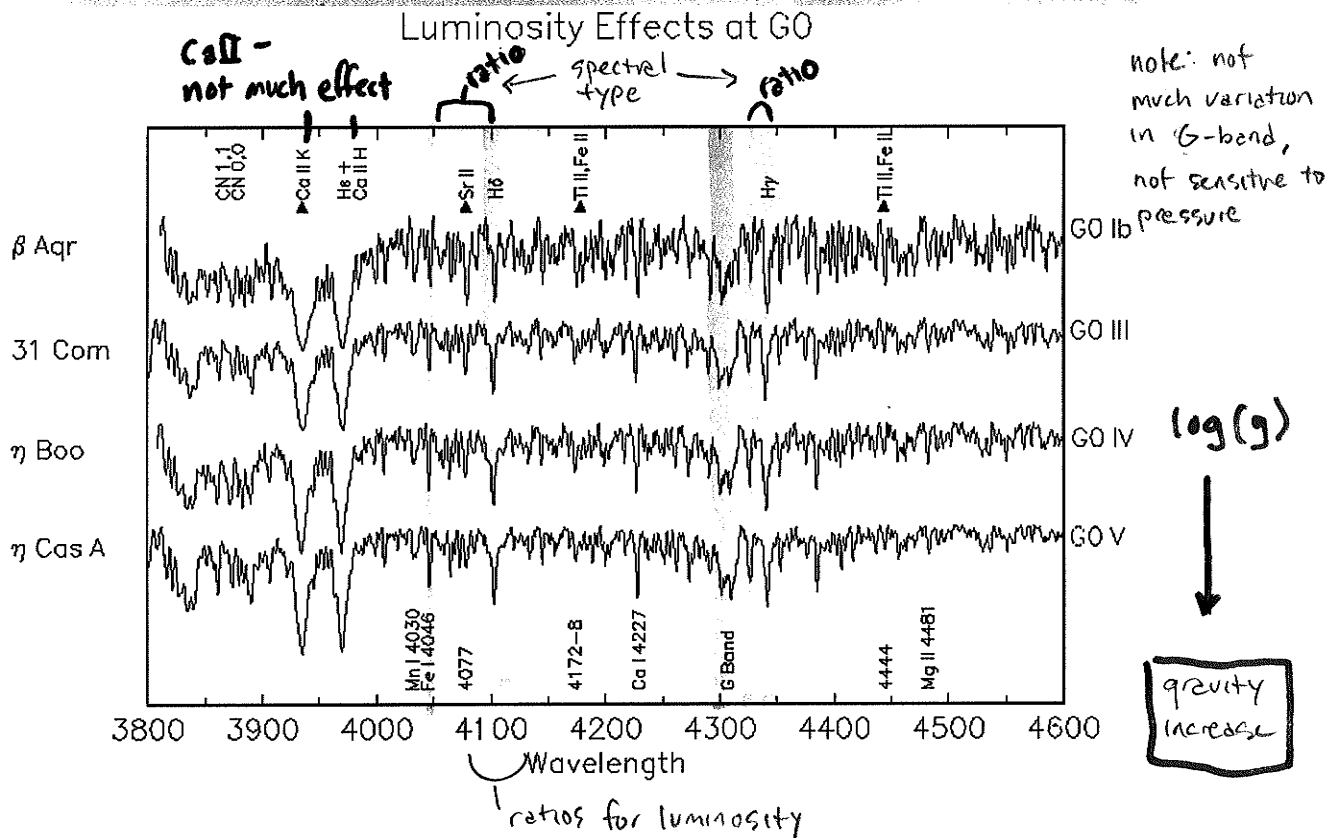
## Luminosity Effects At G0

The spectral type is determined from the ratios  $\lambda\lambda 4045: H\delta$  and  $4325: H\gamma$  for all stars except supergiants. Luminosity differences are shown by the ratios  $\lambda\lambda 4063: 4077$ ,  $4144: 4077$ , and the ratio of the surface intensities of the blends centered near  $\lambda\lambda 4272$  and  $4200$ .



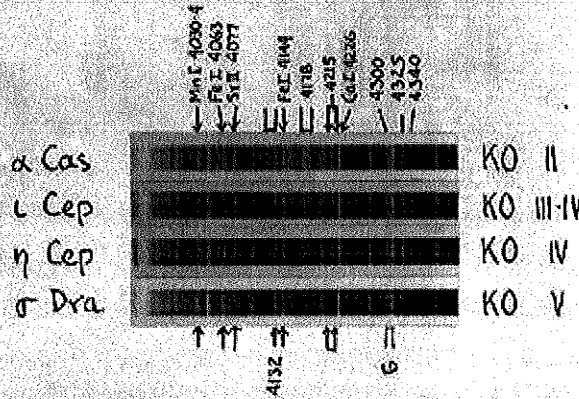
The absolute magnitude of  $\eta$  Boo is about +3.1; that of  $\epsilon$  UMa is about +5.0

Cramer Hi Speed Spectral



## Luminosity Effects At K0

The spectra are classified from the ratios  $\lambda\lambda 4325:4340$  and  $4030.4:4300$  (violet side of G-band). Luminosity differences are shown by the ratios FeI 4063:SiII 4077, FeI 4144:4077 and by the intensity difference of the continuous spectrum on each side of  $\lambda 4215$ .

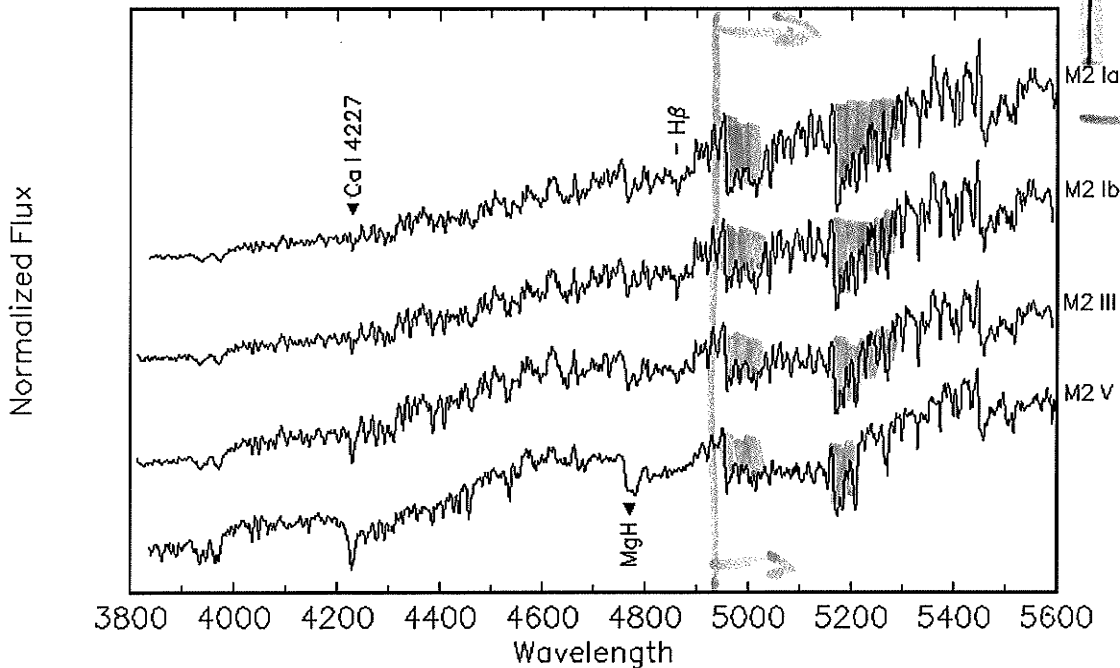


this is bluerward of below graph.

Luminosity differences are also shown by the ratio of the surface intensities of the blends  $\lambda\lambda 4030.4:4178$ . In addition, the broad absorption feature to the violet of FeI 4144 changes in appearance on passing toward the dwarfs and finally degenerates into a fairly well defined line near  $\lambda 4132$ . The ratio of this line to  $\lambda 4077$  shows luminosity differences. Approximate absolute magnitudes are:  $\alpha$  Cas, -1;  $\epsilon$  Cep, +1.5;  $\eta$  Cep, +2.8;  $\sigma$  Dra, +6.1. Cramer Hc Speed Special

↑  
K0  
M2 ↓

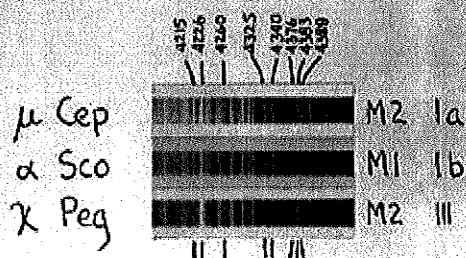
## Luminosity Effects at M2



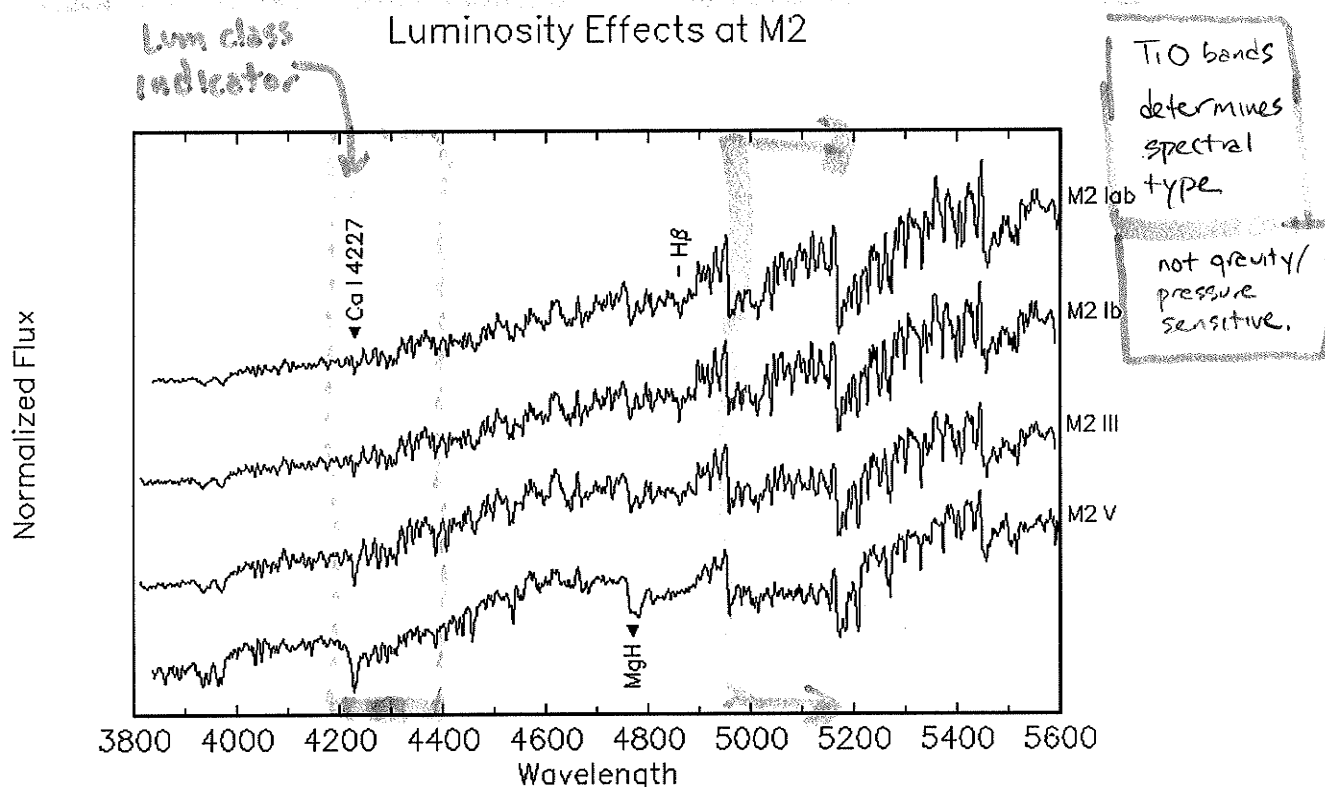
molecular bands unaffected by pressure /  
M2 lab gravity

## Luminosity Effects In The Early M Giants

The spectral types were determined from the intensity of the green TiO bands, which are not shown in the illustration. The line Ca I 4226 has a pronounced negative absolute magnitude effect. The CN break at  $\lambda 4215$  is present in  $\mu$  Cep, possibly faintly present in  $\alpha$  Sco, and probably absent in  $\chi$  Peg.

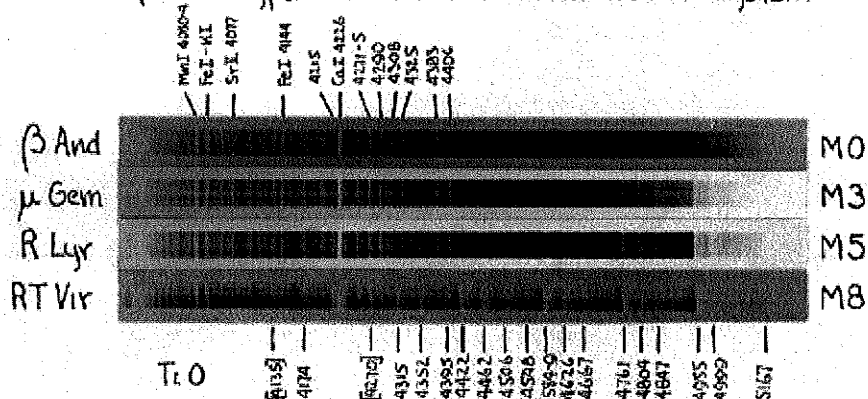


Luminosity line ratios are:  $\lambda\lambda 4215:4260, 4376:4383$ , and  $4389:4383$ . The absolute magnitude of  $\mu$  Cep is probably around  $-6$ , that of  $\alpha$  Sco is near  $-4.0$ .  $\chi$  Peg appears to be an ordinary M giant with an absolute magnitude of about  $0$ .  
Cramer Hi-Speed Special



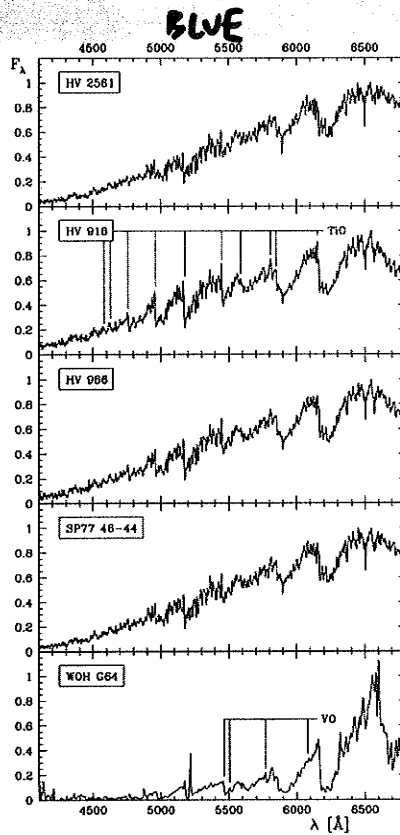
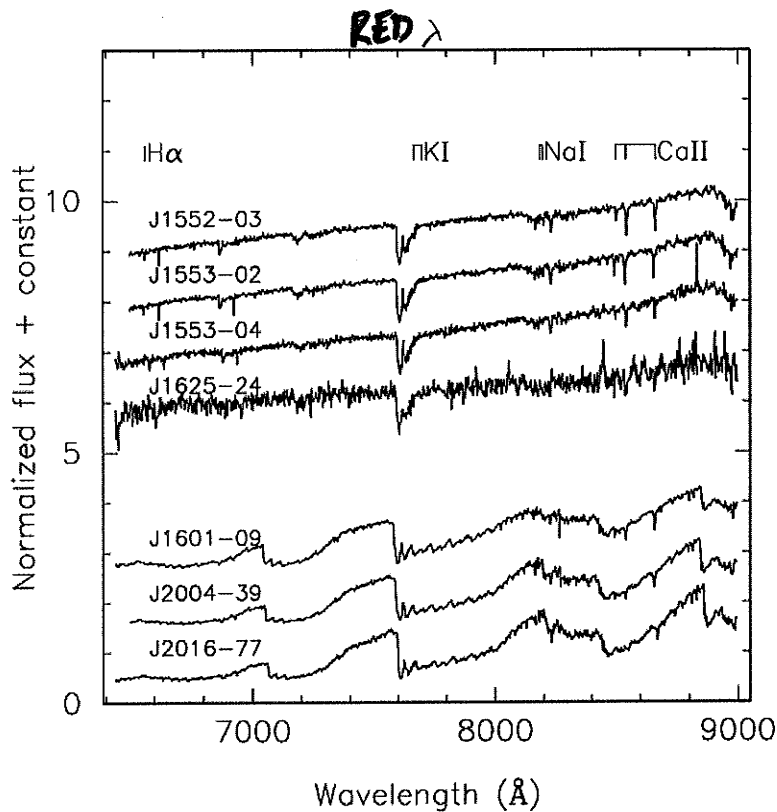
## The M Giant Sequence

The TiO bands appear at M0 and grow uniformly stronger with advancing type. The fainter TiO bands in the blue region become very strong in the latest M classes. The spectral types are on the Mount Wilson system.



The suppression of the blue-green region by TiO is very marked in the advanced M spectra. In the case of  $\alpha$  Virginis the spectral energy distribution in the region  $\lambda\lambda$  4000-5000 simulates a star of considerably higher temperature.

Cramer HC-Speed Special

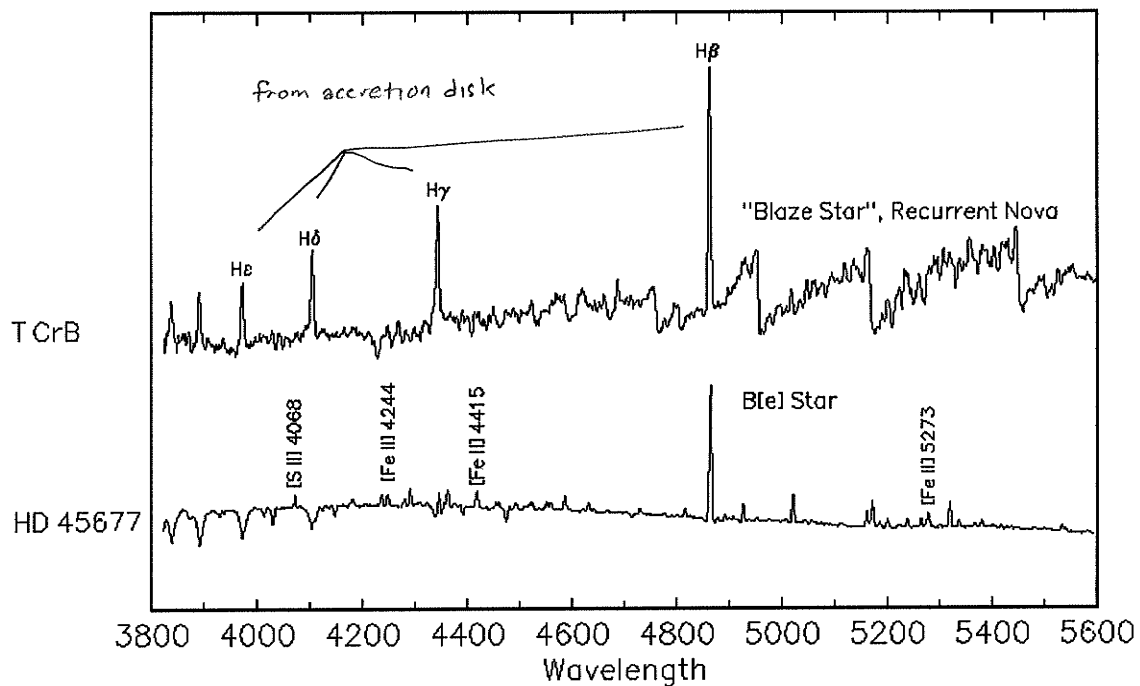




## Emission Line Stars

Two unrelated emission-line stars. The first is the famous "Blaze Star", T CrB, a recurrent nova. This star consists of a cool (as indicated by the presence of TiO bands in the spectrum) component in a binary system with a white dwarf. Gas from the cool component, which fills its Roche lobe, falls onto an accretion disk around the white dwarf. The emission lines are due to hot hydrogen gas in this accretion disk. Material from this disk is accreted onto the surface of the white dwarf. Eventually, this material detonates, producing a dramatic brightening of the system. The second star is a proto-type of the B[e] stars, B-type stars which show forbidden lines in emission. The B[e] stars represent a number of evolutionary states, including supergiants, pre-main sequence stars, compact planetary nebulae and symbiotic stars. The exact nature of HD 45677, illustrated here, is not yet known.

Two Emission-Line Stars  
Normalized Flux



## Herbig Ae Stars

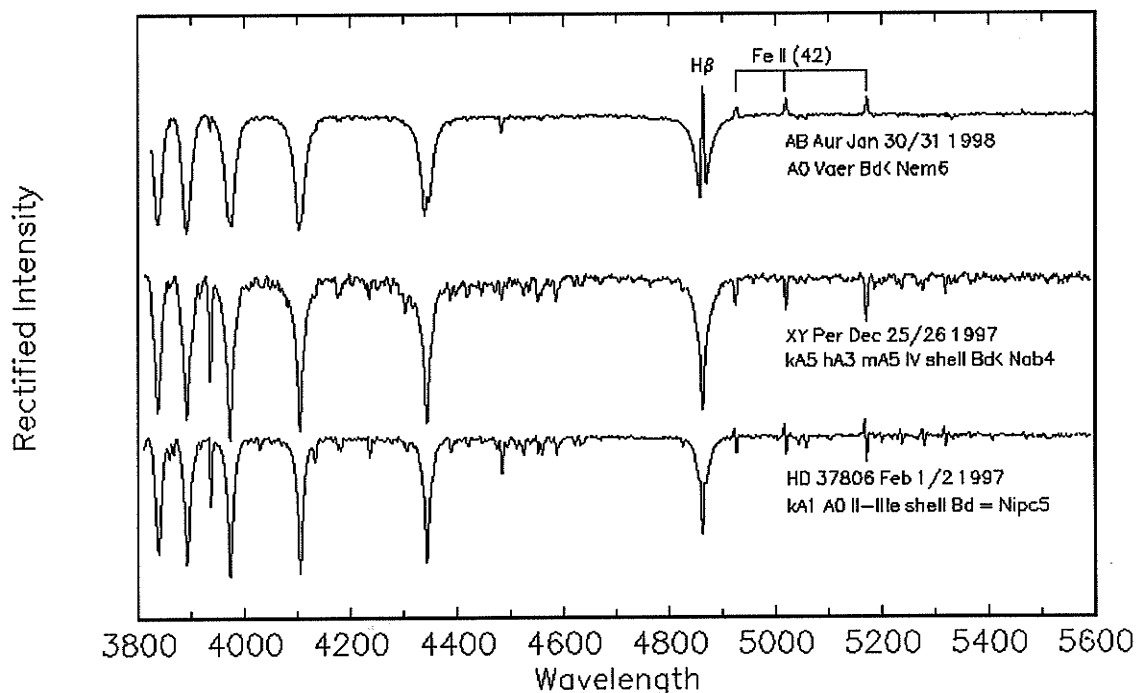
Herbig Ae stars generally show emission in the H line (outside of the spectral range of the spectra used in this atlas), and quite often emission in H and even He. Many Ae stars are still contracting to the main sequence, and are thus either still surrounded by remnants of their stellar cocoons, or have developed massive stellar winds.

The extended spectral type consists of a normal MK type along with an indication of the nature of the Balmer line emission. An "e" indicates strong emission in the H line, (e) indicates marginal or weak emission, and an "r" or "b" indicates whether this emission is shifted to the red or blue of the photospheric line. The strength of the Balmer decrement is indicated by the symbols <, =, > for weak, somewhat weak, normal, somewhat strong, and strong. The nature of the emission and/or absorption, plus the strength relative to the normal absorption strength of the relevant standard of the lines of the Fe II (42) multiplet are indicated with the N index. Nem indicates these lines are in emission, Nab that they are in stronger than normal absorption, and Npc and Nipc indicate P Cygni and inverse P Cygni profiles in these lines.

The spectral types of these Herbig Ae stars can change quite dramatically on time scales of a few days. As a consequence, the spectral types of these stars should always be accompanied by a date.

Fe II lines	$\left\{ \begin{array}{l} \text{Nem} = \text{in emission} \\ \text{Nab} = \text{in absorption} \\ \text{Npc} = \text{P Cygni} \\ \text{Nipc} = \text{inverse P Cygni} \end{array} \right.$	H lines	$\left\{ \begin{array}{l} e = \text{strong emission} \\ (e) = \text{weak emission} \\ "r, b" = \text{emission red/blue shifted} \end{array} \right.$
-------------	--	---------	--

## Herbig Ae Stars

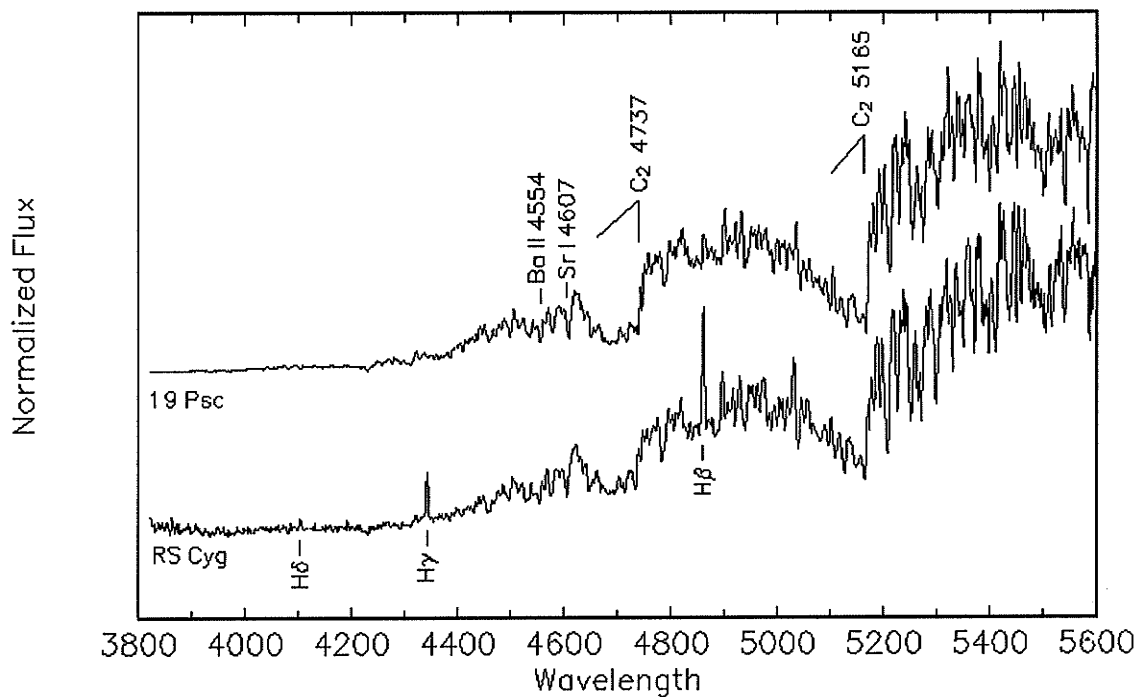


## Carbon Stars

Carbon stars tend to be cool giants (although dwarf carbon stars are known) with greatly enhanced bands of molecules involving carbon. Especially prominent in most carbon stars are the Swan bands of  $C_2$ . Some carbon stars also show enhancements of the G-band (CH) and the CN bands. These two carbon stars show strong lines of barium and strontium, both s-process elements. It is thought that the excess carbon and s-process elements seen in the atmospheres of carbon stars are due to deep convection currents that dredge nuclear-processed material up from the core.

$C_2$  = Swan bands

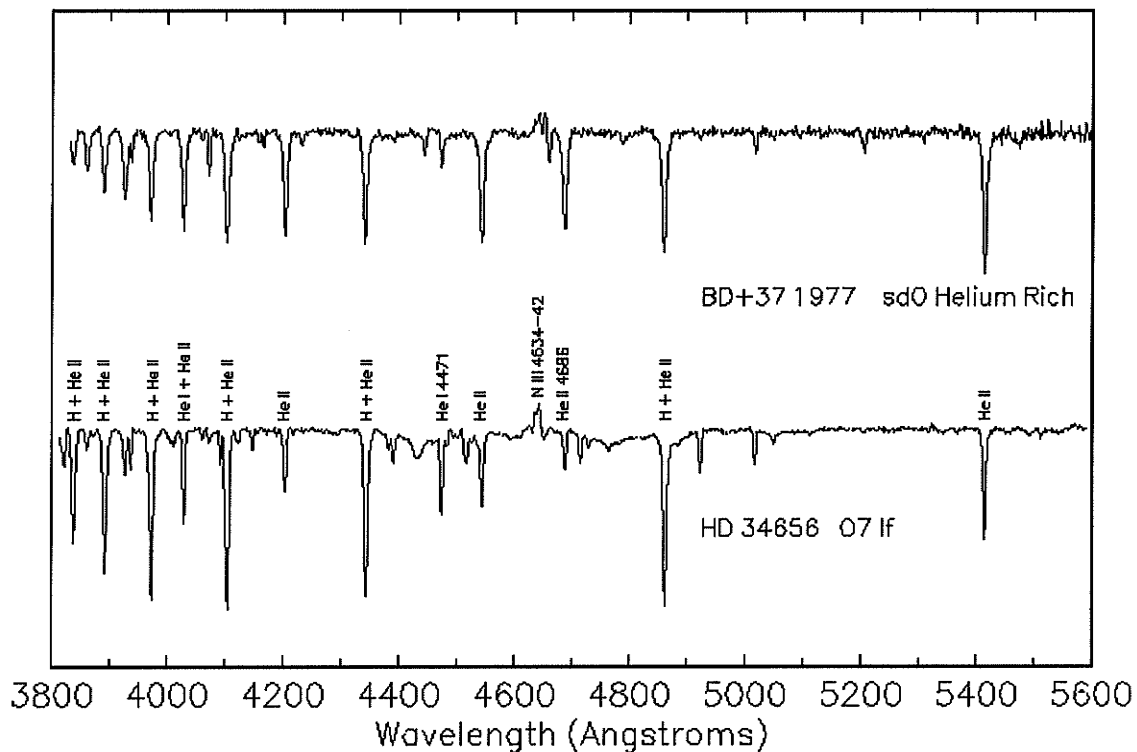
### Two Carbon Stars



## Helium Rich O "sub-dwarf" Star

This is a spectrum of a helium-rich O "subdwarf" star, an extremely hot star which is in the process of evolving into a white dwarf. The near equality of the strengths of the H + He II blends with the He II lines indicates that the atmosphere (and probably the whole of this star) are almost pure helium, with very little if any hydrogen. This star is the exposed core of a star that has thrown off its outer envelope.

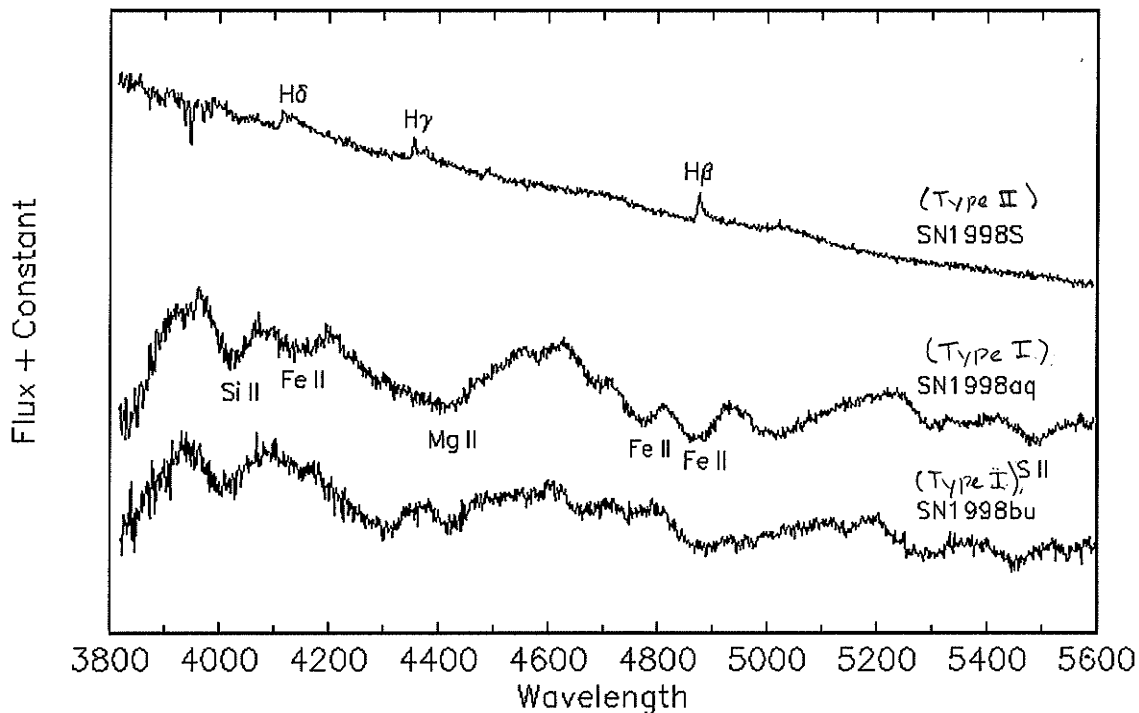
### A Helium-rich Subdwarf



## Supernova from 1998

The spectra of the three bright supernovae of 1998, SN1998S, SN1998aq and SN1998bu. SN1998S is an example of a Type II supernova. The spectra of Type II supernovae are characterized by broad emission lines of hydrogen, usually stronger than can be seen in this particular spectrum of SN1998S (earlier spectra, taken soon after discovery, showed much stronger lines of hydrogen). The catastrophic collapse of this iron core expels the hydrogen-rich envelope, yielding a spectrum dominated by hydrogen. SN1998aq and SN1998bu were both Type I supernovae. The spectra of Type I supernovae are distinguished by broad absorption lines due to ionized metals, and the complete lack of any indication of hydrogen. As a consequence, the progenitors of these supernovae are thought to be binary systems with a carbon-oxygen white dwarf near to the Chandrasekhar limit as one of the components. Material from the other star falls onto the carbon-oxygen white dwarf. When the Chandrasekhar limit is exceeded, the white dwarf undergoes a carbon detonation, producing the supernova explosion. Type I supernovae are more luminous at their maxima than Type II supernovae, have easily recognizable spectra, and thus make excellent standard candles. The metal ions responsible for the broad absorption troughs in the spectrum of SN1998aq have been indicated below the spectrum.

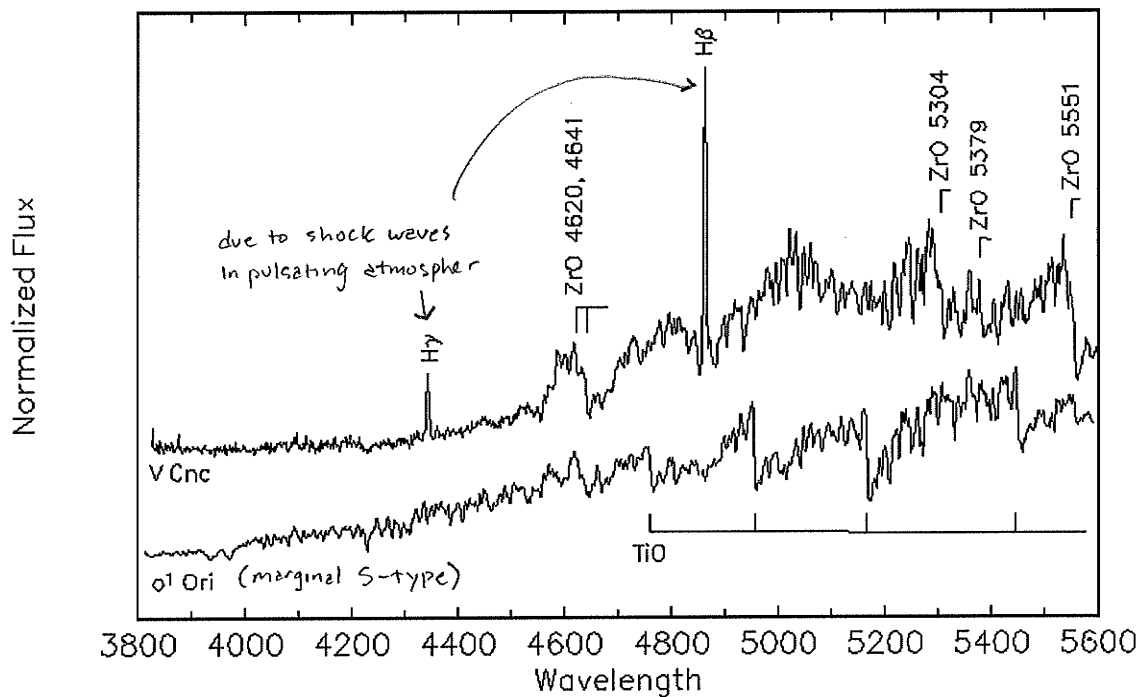
Three Bright Supernovae in 1998



## S Type Stars

S-type stars are defined as cool giants which show evidence of bands of ZrO in their spectra. V Cnc, a semi-regular variable star, shows pronounced bands of ZrO, whereas  $\sigma^1$  Ori is a marginal S-type star, as it shows only marginal evidence of ZrO (see the ZrO bandhead at 5551, barely visible in  $\sigma^1$  Ori). V Cnc shows almost no evidence for TiO in its spectrum, whereas the bands of TiO in  $\sigma^1$  Ori are as strong as those in an M4 giant. The strong hydrogen emission lines in the spectrum of V Cnc are due to shock waves in its pulsating atmosphere. Some S-type stars also show molecular bands due to YO, VO and LaO. The chemical peculiarities in S-type stars are also thought to arise from the dredge-up of nuclear processed material from deep within the star.

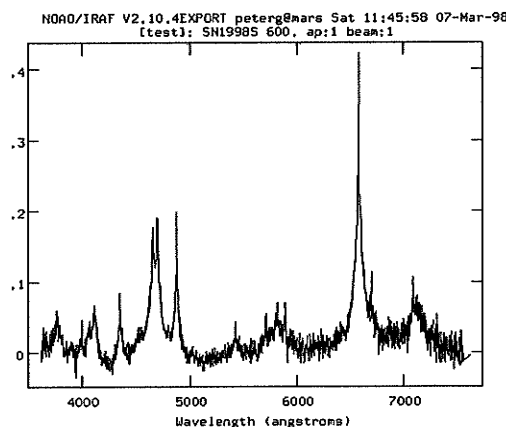
Two S-type Stars



## Wolfe Rayet Stars

Wolf Rayet stars represent an evolutionary phase in the lives of massive stars during which they undergo heavy mass loss. They are characterized by an extraordinary spectrum that is dominated by emission lines of highly ionized elements. Recent general reviews on Wolf-Rayet stars have been made by Abbott & Conti (1987), Willis (1987, 1991), Conti & Underhill (1988), Smith (1991a), van der Hucht (1991, 1992), Maeder (1991c), and Massey & Armandroff (1991). W-R stars are considered "bare cores" resulting mainly from stellar winds peeling off of single stars initially more massive than about 25 to 40  $M$ . Close binaries might also lose their outer layers from Roche lobe overflow. The main evidence for the bare core model as reviewed by Lamers et al (1991) are the following:

- H/He ratios in W-R stars are low or zero.
- The CNO ratios are typical of nuclear equilibrium.
- The continuity of the abundances in the sequence of types O, Of, WNL, WNE, WCL, WCE, and WO corresponds nicely to a progression in peeling off the outer material from evolving massive stars.
- The observed winds in progenitor O stars and in supergiants are high enough to remove the stellar envelopes within the stellar lifetimes. Also, the average winds in W-R stars (Conti 1988) are able to accomplish further significant mass loss.
- W-R stars have low average masses (between 5 and 10  $M$ ; Abbott & Conti 1987); moreover, they fit well the mass-luminosity relation for He stars (Smith & Maeder 1989).
- W-R stars are present in young clusters and associations with ages smaller than 6 Myr (Humphreys & McElroy 1984, Schild & Maeder 1984).
- He- and N-rich shells are present around some W-R stars (Esteban & Vilchez 1991).
- With their bright emission lines and their high luminosities, W-R stars are observable at large distances and are thus the stars for which we have the best sampling in other galaxies. Their emission lines also can become visible in the integrated spectrum of galaxies with active star formation, which enables us to extend the studies of young massive stars even farther out in the Universe.





## Metallicity Effects in Massive Stars

1. **Nuclear production.** Metallicity  $Z$  may influence the nuclear rates; a good example occurs for the CNO cycle. A very slight contraction or expansion to a new equilibrium state may compensate for a change in nuclear rates (Schwarzschild 1958). In massive stars, a lower  $Z$  also produces a more active H-burning shell in the post-main sequence evolution and this favors a blue location in a part or the whole of the He-burning phase (Brunish & Truran 1982a, b; Schaller et al 1992). This was one of the initial explanations proposed for the blue precursor of SN 1987A (Truran & Weiss 1987).
2. **Opacity effects.** In the interiors of massive stars, electron scattering, which is independent of  $Z$ , is the main opacity source. Thus, in contrast to the case of low and intermediate mass stars, metallicity has no great direct effect on the inner structure of massive stars.
3. **Stellar winds.** In the very external layers,  $Z$  may strongly influence the opacity and thus the atmospheres and winds. Wind models for O stars by Abbott (1982) suggested a  $Z$ -dependence of the mass loss rates of the form  $\dot{M} \propto Z^{-1}$ , with  $\alpha = 1.0$ . Other models gave a value of between 0.5 and 0.7 (Kudritzki et al 1987, 1991; Leitherer & Langer 1991; Kudritzki 1994). It is likely that this is the main effect by which  $Z$  may influence massive star evolution (Maeder 1991a). For yellow and red supergiants, there are no models (Lafon & Berruyer 1991) nor observations (Jura & Kleinmann 1990) giving reliable vs  $Z$  information; thus a major uncertainty in post-MS evolution remains.
4. **Helium content.** A ratio  $Y/Z$  greater than 3 between the relative enrichments in helium and heavy elements has been established from low- $Z$  H II regions (Peimbert 1986, Pagel et al 1992). Thus, changes in  $Z$  imply large changes in  $Y$ , which have a direct effect on the models.

